MRS Communications (2017), 1 of 5

doi:10.1557/mrc.2017.119

MRS Communications

Research Letter

Ice-templated silicon foams with aligned lamellar channels

Q1 **Fernando L. Reyes Tirado, Jiaxing Huang,** and **David C. Dunand,** Department of Materials Science and Engineering, Northwestern University, 2220 Campus Dr., Evanston, Illinois 60208, USA

Address all correspondence to David C. Dunand at **dunand@northwestern.edu**

(Received 8 September 2017; accepted 11 October 2017)

Abstract

An aqueous suspension of 5 vol% silicon (Si) nanoparticles was directionally solidified at substrate temperatures between −10 and −25 °C, resulting in colonies of aligned pure ice dendrites separated by interdendritic Si particles packed walls. Channels are created by sublimation of the dendrites, and the surrounding Si walls are densified by sintering. The resulting Si foams exhibit a 76 ± 2% macroporosity, with the width of the ice-templated channels and the Si walls decreasing with solidification temperature, from 106 to 60 μm and from 34 to 17 μm, respectively. Si walls show high surface roughness from inverse templating of short secondary ice dendrite arms.

Introduction

Ice templating is a directional solidification technique that allows the creation of materials with directional, anisotropic channels or pores which, if designed appropriately (e.g., slow directional solidification with very fine powders that are partially sintered), provide high surface area and high gas permeability. In this technique, particles suspended in a liquid (usually water) are pushed by, and concentrated between, solid dendrites (usually ice) growing along an applied thermal gradient into colonies of parallel lamellar dendrites.[1,2] Particles pushed between the dendrites form lamellar structures (walls) that are inverse-templated from the ice lamellar dendritic structure.[3] Sublimation of the ice creates a porous green body with aligned lamellar channels and walls; sintering promotes wall densification without elimination of the channels.[1,4] This technique has gained considerable attention due to its facile implementation and its ability to tailor micro- and macrostructures (and the associated mechanical and physical properties), such as channel and wall volume fraction, spacing, width, orientation, and surface morphology, as well as microporosity within sintered walls. Because of this flexibility, ice templating has been used to create foams with directional porosity from ceramic,[4] metallic,[5–10] polymeric,[11] and biologic materials,[12] as reviewed in Deville's monograph.[1] The literature does not report silicon (Si) ice templating,[1] with the exception of two recent articles which describes silicon nitride (Si_3N_4) foams created by nitriding and sintering of ice-templated, freeze-dried Si particle foams, with non-directional[13] and directional[14] solidification. In the latter study, the authors focus on the Si_3N_4 foams and report little on the precursor Si particle structures directionally solidified at 25 μm/s: they show micrographs of lamellar walls, consisting of ~7 μm Si particles bound with polyvinyl alcohol, before heat treatment under nitrogen at 1350–1450 °C to sinter and nitride them to Si_3N_4.[14]

Si is attracting considerable attention as an anode material for Li-ion batteries due to its low discharge potential and high charge capacity (4200 mAh/g).[15,16] Furthermore, the low discharge potential exhibited by Si anodes can help avoid lithium (Li) plating and the formation of Li dendrites, which are often a safety concern. The use of Si anodes, however, is limited due to extreme volume changes (~400%) during (de)lithiation cycles,[15,17,18] and the low diffusion rate of Li ions in Si at high charge rates.[15] Creating Si anodes with submicron dimensions and open porosity is a very promising approach to accommodating the volume changes encountered during (de)lithiation cycling.[15,17–19] Moreover, (de)lithiation cycling kinetics can be enhanced by a reduction in diffusion lengths.[16] However, existing methods for processing of porous, nanostructured Si are complex and thus expensive. Recently, studies have shown that sludge recovered from Si wafer cutting processes could be purified and recycled to obtain high-purity Si powders.[20] These recycled powders, in the form of a cast slurry after mixing with active materials, can then be reused to create anodes for Li-ion batteries in a sustainable manner and at relatively low cost,[19] but the accommodation of large strains remains a problem, leading to capacity fading and electrode failure. We envision porous Si structures, created by the above method of freeze casting and sintering, as a solution to the problem of damage accumulation of Si anodes, with the following characteristics: (i) high porosity and small feature sizes (accommodating large strains and thus resisting pulverization); (ii) directional porosity (encouraging rapid diffusional flow in the electrolyte); (iii) continuous structure (achieving low electronic resistivity, unlike Si powder beds); and (iv) high surface area (enabling rapid reaction with Li).

In this work, we describe directional freeze casting of 5 vol% Si colloidal suspensions to achieved sintered Si foams with directional aligned channels and walls, and we study the effects of solidification temperature on the foams microstructure. Here, we employ commercially available Si nanopowders as the model system, but recycled Si powder[19] could be used at a later stage to reduce price and improve the sustainability of these foams.

Experimental methods

Colloidal Si suspensions in deionized water were prepared by using Si nanoparticles (<100 nm, Sigma–Aldrich Co., St Louis, MO, USA), poly (ethylene glycol) (PEG, Sigma–Aldrich Co., avg. Mn: 400) as binder, and ethylene glycol (Consolidated Chemical & Solvents, Quakertown, PA, USA) and Zephrym™ PD4974-LQ-(MH) (CRODA, Columbus, NJ, USA) as dispersants. PEG (2.0 wt% with respect to Si dry powder mass) was dissolved into ~2.5 mL of deionized water with ethylene glycol (2.0 wt% with respect to Si dry powder mass) and stirred for 15 min. Using a separate container, 5 vol% of Si powder (with respect to total volume of deionized water, corresponding to 10.9 wt%) was added to ~7 mL of water and Zephrym (2.0 wt% with respect to Si) and stirred in a vortex mixer for 5 min. Both mixtures were then combined and roll-milled for 48 h at 60 rpm in a Teflon container with yttria-stabilized zirconia spheres.

The colloidal suspensions were poured into insulating cylindrical Teflon molds (26 mm in height and 15.6 mm in inside diameter), to a height of ~13 mm, sealed on the bottom with a thin aluminum foil with high thermal conductivity. The molds containing the colloidal suspension were then placed on a thermoelectric cooling device pre-cooled to −10, −15, −20, or −25 °C. To favor a vertical temperature gradient, the top and sides of the Teflon molds were insulated with polystyrene foam. Once solidification was complete, frozen samples were removed from the mold and placed in a freeze dryer for sublimation (48 h at a collector temperature of −40 °C and a pressure of 0.133 mbar).

The ice-templated green bodies were transferred to a tube furnace (MTI Corporation GSL-1500X-50HG) for sintering under hydrogen atmosphere (99.999% pure H_2 gas) in a two-stage process: (i) a binder- and dispersant burnout stage at 300 °C for 1 h; and (ii) a sintering stage at 1300 °C for 4 h. The heating and cooling temperature ramps were 10 and 5 °C/min, respectively. The sintered samples were cut with a razor blade and longitudinal and radial cross-sections were impregnated with epoxy resin, grinded using 320, 400, 600, 800, 1200 grit SiC paper, polished using 6, 3, and 1 μm diamond suspension, and imaged via optical and scanning electron microscope (SEM). ImageJ was used to measure porosity, wall width, and channel width on the cross-sections. Wall and channel widths were determined using the line-intercept method with measurements taken at the top quarter of the foam. Bright gray regions in the SEM micrographs were identified as walls and dark regions infiltrated with epoxy were identified as channels. The number of measurements, per sample, for wall and channel width was in the range of 65–143.

Results and discussion

Microstructure

Si suspensions were solidified using freezing substrate temperatures of −10, −15, −20, and −25 °C, sublimated and then sintered. Sintered foams, shown in Fig. 1, are ~12 mm in diameter and 5–7 mm in height, and they display colonies of directional lamellar channels and walls aligned along the vertical solidification direction. Macroscopic volumetric shrinkage was ~63%, with radial shrinkage of ~24%, in general agreement with other ceramic ice-templated structures, where linear shrinkage due to sintering is ~20–30%.[1]

Figures 2(a)–2(h) show SEM micrographs of polished cross-sections, taken in the top quarter of the foam, parallel and perpendicular to the freezing direction, for the four solidification temperatures. Figures 2(a)–2(d) show representative images of the channel/wall morphology parallel to the freezing direction. It is apparent from these micrographs that a decreasing freezing substrate temperature is associated with thinner ice dendrites, and thus thinner channels. This trend is consistent with the literature, where it is well established that, as the solidification temperature decreases, the freeze front velocity increases, promoting the growth of thinner ice dendrites.[1,4,7] At lower solidification temperatures, undercooling increases, producing a higher number density of ice crystals. Once nucleation occurs, initial ice growth is very rapid due to the high

Fig. 1 - Colour online, Colour in print

Figure 1. Ice-templated Si foam after sintering displaying lamellar porosity. Solidification temperature varied from left to right: −10, −15, −20, and −25 °C. The same volume of suspension was used to solidify all samples.

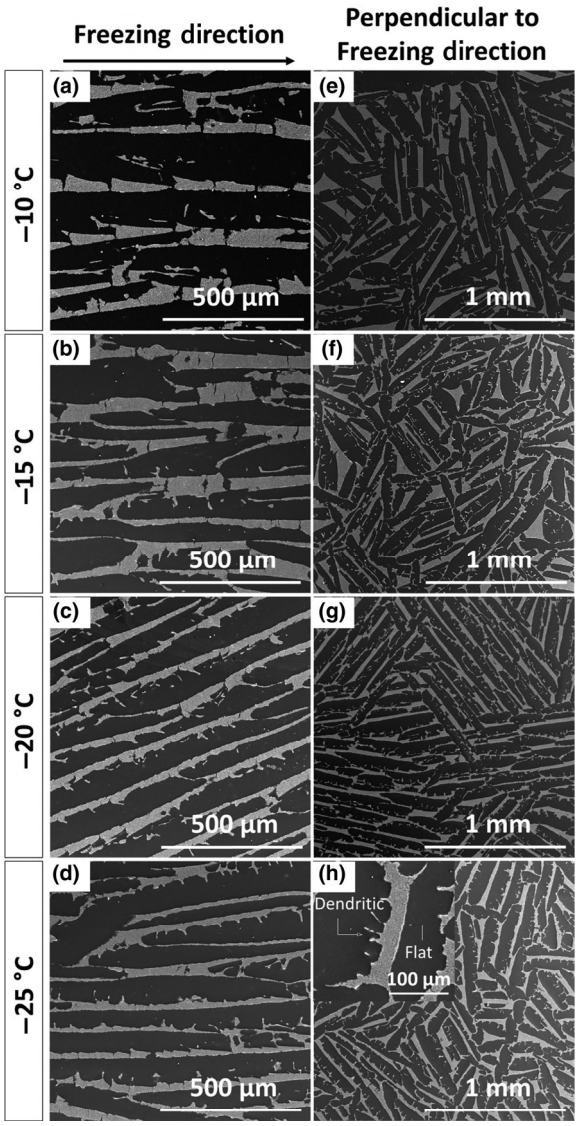

Fig. 2 - B/W online, B/W in print

Figure 2. SEM micrographs of longitudinal (a–d) and perpendicular (e–h) cross-sections of sintered foams as a function of solidification temperature. Brighter regions represent sintered silicon walls and dark areas represent channels. Insert in bottom right micrograph shows wall surfaces (rough on one side and smooth on the other).

undercooling, resulting in thinner ice dendrites. Moreover, the structure of the Si walls, which are inversely templated by the original ice dendrites, is representative of ice lamellae/dendritic growth, where one side of the ice primary dendrites shows the presence of secondary dendrite arms, while the other has a flat interface. The formation of secondary ice dendrites on only one of the two main surfaces of the lamellar primary dendrites is due to a slow growth velocity perpendicular to the solidification direction and a small tilt of the primary ice dendrites, commonly observed for ice templating of aqueous ceramic suspensions.[1,4] Therefore, it is expected that the growth velocity of secondary arm dendrites will increase as the freeze front

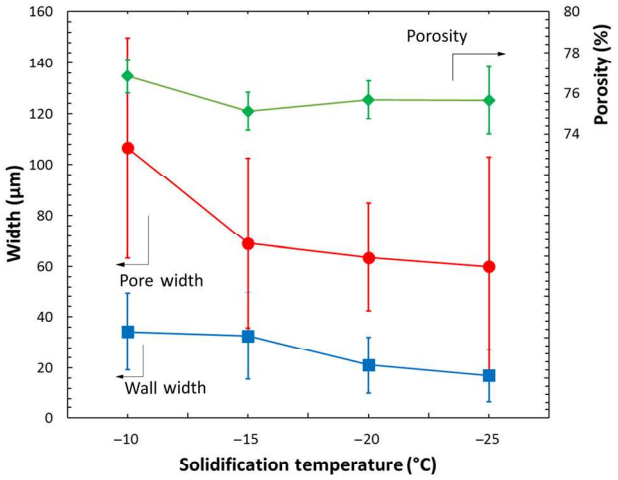

Fig. 3 - Colour online, Colour in print

Figure 3. Plot of channel width, Si wall width, and foam porosity versus solidification temperature.

velocity increases. Figures 2(e)–2(h) show representative perpendicular cross-section illustrating the increase of one-sided secondary arm dendrites with decreasing solidification temperature.

Longitudinal cross-sections of the Si foams were used to determine the average channel and wall width, while perpendicular cross-sections were used to determine the average macroporosity: Fig. 3 shows these parameters as a function of freezing temperature. The porosity stays constant at ~76% as expected, given the constant Si particle volume fraction in the suspension.[1,21] While porosity in the sintered structures is independent of solidification temperature, both channel and wall widths decrease with decreasing temperature (Fig. 3). Specifically, the average channel width decreases from 106 ± 43 µm at a solidification temperature of −10 °C to 60 ± 42 µm at a solidification temperature of −25 °C, almost a factor 2. The inversely templated Si walls exhibit the same trend, with the average wall width being halved from 34 ± 15 to 17 ± 10 µm with lower solidification temperatures.

Figures 4(a) and 4(b) show SEM micrographs of the fracture surface of a sintered Si foam ice-templated at −10 °C and the microstructure of a Si wall solidified at −15 °C, respectively. In Fig. 4(a), Si walls with different orientations are visible. A wall with a flat side, as seen in Fig. 2, is shown on the left side of the micrograph, delineated with dashed lines. A wall with the rougher surface (inversely templated from the ice secondary dendrite arms) is visible on the right side of the micrograph, as indicated by dotted lines. Some cracks are evident in the densified walls, which may have been created by ice lenses formed during solidification,[1] sintering shrinkage or by sectioning.

Figure 4(b) illustrates a nearly fully dense Si wall. Some microporosity within the wall is present, but the two surfaces of the wall are nearly dense over a depth of 1–2 µm. We observed 128 randomly selected Si walls: 73% of the walls

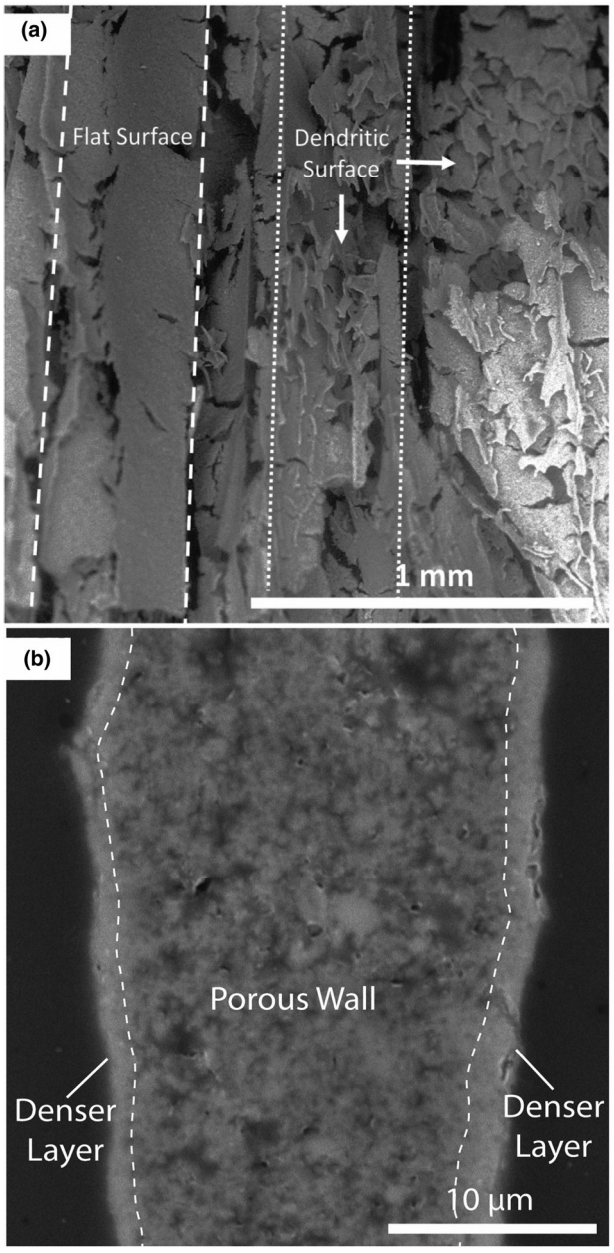

Fig. 4 - B/W online, B/W in print

Figure 4. (a) SEM micrograph of a fracture surface from a sintered Si foam, displaying wall microstructure and pore channels. (b) SEM micrograph of a longitudinal cross-section showing microporosity within a wall with a dense layer at the wall surface.

showed, on one or both of their surfaces, a similar 1–2 µm thin region which was nearly fully dense, while the remaining walls had no, or only a partial, densified surface region. This surface densification may reflect the accumulation of silica created by the reaction of residual oxygen in the sintering atmosphere. Previous studies have shown that a silica layer on fine Si particles (<100 nm) helps densification at high temperatures (>1100 °C) by promoting lattice diffusion, which contributes to densification, at the expense of surface diffusion, which does not.[22] Moreover, experiments in which the silica layer has been reduced do not display densification beyond 65% relative density for a sintering time of 3 h at 1315 °C (with a particle size of 220 nm).[22] The presence of silica on the surface of our powders, therefore, could be a key to achieving highly densified Si walls. This suggests that the sintering kinetics and residual microporosity of ice-templated Si foams can be further tuned by adjusting the water vapor pressure in the furnace, besides the usual sintering parameter of time, temperature and particle size.

Si foams as precursors

While the motivation of this study was to create porous, lamellar Si structures for Li-ion battery applications, ice-templated Si foams may be used as a precursor for various other compounds, including silicon carbide (SiC), nitride and oxides, and metal silicides. Gas-phase nitridation is a well-established method to create Si_3N_4.[13] Si_3N_4 foams created via various methods (e.g., freeze casting of Si_3N_4 powders, direct Si powder nitridation and sintering, emulsions and reduction–nitridation of silica) exhibit high surface area, good thermal shock resistance, high thermal conductivity, high gas permeability, and excellent high-temperature strength for applications such as heat exchangers, catalyst and filter.[13,23–26] All these properties are improved by the directional interconnected channel structure inherent to directional freeze casting. Similarly, SiC foams could be created via carburization of freeze-cast Si foams: such carburization is rapid on small features; as demonstrated previously on Si nanopillars,[27] SiC foams have also been created by freeze casting of SiC particles and sintering at 1800–1900 °C,[28] or by freeze casting of polycarbosilane/camphene solution, followed by decomposition. Further examples of freeze-cast Si_3N_4, SiC and SiO_2 are summarized in Deville's monograph.[1] Finally, gas-phase reaction with metal precursors—e.g., halides based on refractory metals such as Cr, Nb, Mo, Ta, W—could be used to transform, partially or fully, the Si to the corresponding silicide, resulting in a foam with a much higher melting point than Si and high-temperature strength and ductility.

Furthermore, a freeze-cast Si foam could be infiltrated with a liquid metal or alloy, e.g., a eutectic Al-12%Si melt which is at chemical equilibrium with Si, thus avoiding dissolution or reaction of the Si walls. This approach was taken for the infiltration of packed Si powders by liquid aluminum.[29] Such an interpenetrating Si/Al-12Si composite will display an unusual combination of low thermal expansion and high thermal conductivity (useful for electronic substrates), as well as low density, high wear resistance, and high specific strength and stiffness (useful for structural applications). This concept was recently applied to ice-templated tungsten foams, infiltrated with liquid copper to create W/Cu composites with anisotropic electrical conductivity.[30]

Conclusions

Here, we demonstrate ice templating of 5 vol% Si colloidal aqueous suspensions to produce Si foams with directionally

aligned lamellar channels, after ice removal and sintering. The following conclusions are drawn:

The macroporosity of the freeze-dried Si powder foams is reduced from 95% to ~76% after sintering, while volumetric shrinkage of the samples is ~63%. The Si walls are nearly fully sintered, likely due to the role of silica in aiding densification.

The macroporosity of the sintered foams, ~76%, is unaffected by changes in the solidification temperature. By contrast, the width of the channels decreases with decreasing temperature, due to faster freeze front velocities. The width of the Si walls concurrently decreases too.

The channel morphology, which is templated from the ice dendrites, is consistent with that of other ice-templated ceramic systems such as alumina or Si_3N_4, where secondary dendrite arms grow on only one side of the ice crystals.

These Si foams provide a platform for studying the properties of Si with directional anisotropic pores created by ice templating, offer promise for energy applications such as battery electrodes, and may further be processed into carbide, nitride, oxide and silicide foams.

Acknowledgments

This study was supported by the National Science Foundation (NSF) via CMMI-1562941 (September 2016-January 2017). F.L.R.T also acknowledges the support of a NSF Graduate Research Fellowship. This work made use of the EPIC facility of Northwestern University's *NUANCE* Center, which has received support by NSF ECCS-1542205 and DMR-1121262; and the Materials Characterization and Imaging Facility supported by NSF DMR-1121262. F.L.R.T acknowledges experimental assistance from Mr. Ritij Goel, Ms. Kristen Scotti, and Ms. Shannon L. Taylor (Northwestern University). Useful discussions with Ms. Kristen Scotti are acknowledged.

References

1. S. Deville: *Freezing Colloids: Observations, Principles, Control, and Use* (Springer International Publishing, Cham, 2017).
2. R. Liu, T. Xu, and C. an Wang: A review of fabrication strategies and applications of porous ceramics prepared by freeze-casting method. *Ceram. Int.* 2907 (2015).
3. K.L. Scotti, E.E. Northard, A. Plunk, B.C. Tappan, and D.C. Dunand: Directional solidification of aqueous TiO_2 suspensions under reduced gravity. *Acta Mater.* 608 (2017).
4. S. Deville: Freeze-casting of porous ceramics: a review of current achievements and issues. *Adv. Eng. Mater.* 155 (2008).
5. H. Jo, M.J. Kim, H. Choi, Y.-E. Sung, H. Choe, and D.C. Dunand: Morphological study of directionally freeze-cast nickel foams. *Metall. Mater. Trans. E*, 46 (2016).
6. R. Sepúlveda, A.A. Plunk, and D.C. Dunand: Microstructure of Fe_2O_3 scaffolds created by freeze-casting and sintering. *Mater. Lett.* 56 (2015).
7. Y. Chino, and D.C. Dunand: Directionally freeze-cast titanium foam with aligned, elongated pores. *Acta Mater.* 105 (2008).
8. A.A. Plunk, and D.C. Dunand: Iron foams created by directional freeze casting of iron oxide, reduction and sintering. *Mater. Lett.* 112 (2017).
9. H. Park, M. Choi, H. Choe, and D.C. Dunand: Microstructure and compressive behavior of ice-templated copper foams with directional, lamellar pores. *Mater. Sci. Eng. A* (August 2016), 435 (2017).
10. A. Röthlisberger, S. Häberli, R. Spolenak, and D.C. Dunand: Synthesis, structure and mechanical properties of ice-templated tungsten foams. *J. Mater. Res.* 753 (2016).
11. H. Schoof, L. Bruns, A. Fischer, I. Heschel, and G. Rau: Dendritic ice morphology in unidirectionally solidified collagen suspensions. *J. Cryst. Growth* 122 (2000).
12. S. Deville: Freeze-casting of porous biomaterials: structure, properties and opportunities. *Materials* (*Basel*) 1913 (2010).
13. H.L. Hu, Y.P. Zeng, Y.F. Xia, D.X. Yao, and K.H. Zuo: High-strength porous Si_3N_4 ceramics prepared by freeze casting and silicon powder nitridation process. *Mater. Lett.* (1295), 285 (2014).
14. D.S. Kim, and D.K. Kim: Hierarchical structure of porous silicon nitride ceramics with aligned pore channels prepared by ice-templating and nitridation of silicon powder. *Int. J. Appl. Ceram. Technol.* 921 (2015).
15. M. Ge, X. Fang, J. Rong, and C. Zhou: Review of porous silicon preparation and its application for lithium-ion battery anodes. *Nanotechnology* 422001 (2013).
16. J.-K. Yoo, J. Kim, H. Lee, J. Choi, M.-J. Choi, D.M. Sim, Y.S. Jung, and K. Kang: Porous silicon nanowires for lithium rechargeable batteries. *Nanotechnology* 424008 (2013).
17. M.P.B. Glazer, J. Cho, J. Almer, J. Okasinski, P.V. Braun, and D.C. Dunand: In operando strain measurement of bicontinuous silicon-coated nickel inverse opal anodes for Li-ion batteries. *Adv. Energy Mater.* 1 (2015).
18. C.K. Chan, H. Peng, G. Liu, K. McIlwrath, X.F. Zhang, R.A. Huggins, and Y. Cui: High-performance lithium battery anodes using silicon nanowires. *Nat. Nanotechnol.* 31 (2008).
19. H.D. Jang, H. Kim, H. Chang, J. Kim, K.M. Roh, J.-H. Choi, B.-G. Cho, E. Park, H. Kim, J. Luo, and J. Huang: Aerosol-assisted extraction of silicon nanoparticles from wafer slicing waste for lithium ion batteries. *Sci. Rep.* 9431 (2015).
20. H.D. Jang, H. Kim, D.S. Kil, and H. Chang: A Novel recovery of silicon nanoparticles from a waste silicon sludge. *J. Nanosci. Nanotechnol.* 2334 (2013).
21. J. Seuba, S. Deville, C. Guizard, and A.J. Stevenson: Gas permeability of ice-templated, unidirectional porous ceramics. *Sci. Technol. Adv. Mater.* 313 (2016).
22. J.M. Lebrun, A. Sassi, C. Pascal, and J.M. Missiaen: Densification and microstructure evolution during sintering of silicon under controlled water vapor pressure. *J. Eur. Ceram. Soc.* 2993 (2013).
23. L. Yin, X. Zhou, J. Yu, and H. Wang: Preparation of high porous silicon nitride foams with ultra-thin walls and excellent mechanical performance for heat exchanger application by using a protein foaming method. *Ceram. Int.* 1713 (2016).
24. Y. Xia, Y.-P. Zeng, and D. Jiang: Microstructure and mechanical properties of porous Si3N4 ceramics prepared by freeze-casting. *Mater. Des.* 98 (2012).
25. S.-Y. Shan, J.-F. Yang, J.-Q. Gao, W.-H. Zhang, Z.-H. Jin, R. Janssen, and T. Ohji: Porous silicon nitride ceramics prepared by reduction-nitridation of silica. *J. Am. Ceram. Soc.* 2594 (2005).
26. E.G. de Moraes, and P. Colombo: Silicon nitride foams from emulsions. *Mater. Lett.* 128 (2014).
27. M. Ollivier, L. Latu-Romain, and E. Latu-Romain: Growth of a 3C-SiC layer by carburization of silicon nanopillars. *Mater. Lett.* 263 (2015).
28. V. Naglieri, H.A. Bale, B. Gludovatz, A.P. Tomsia, and R.O. Ritchie: On the development of ice-templated silicon carbide scaffolds for nature-inspired structural materials. *Acta Mater.* 6948 (2013).
29. Y. Chen, and D.D.L. Chung: Silicon-aluminium network composites fabricated by liquid metal infiltration. *J. Mater. Sci.* 6069 (1994).
30. A. Röthlisberger, S. Häberli, H. Galinski, D.C. Dunand, and R. Spolenak: Ice-templated W-Cu composites with high anisotropy. 1 (2017). arXiv:1708.06801.